Survey and Assessment of Available Measurements on Thermodynamic Properties of the Mixture {Water+Ammonia}

Cite as: Journal of Physical and Chemical Reference Data **27**, 45 (1998); https://doi.org/10.1063/1.556014
Submitted: 04 March 1997 . Published Online: 15 October 2009

Reiner Tillner-Roth, and Daniel G. Friend

Survey and Assessment of Available Measurements on Thermodynamic Properties of the Mixture {Water+Ammonia}

Reiner Tillner-Roth[a] and Daniel G. Friend

National Institute of Standards and Technology, Physical and Chemical Properties Division, 325 Broadway, Boulder, Colorado 80303

Received March 4, 1997; final manuscript received October 30, 1997

Mixtures of water and ammonia play an important role in absorption refrigeration cycles and have received attention as working fluids in modern power generation cycles. For design and simulations during the development of any application, the thermodynamic properties have to be known accurately. Measurements of available thermodynamic data are compiled and summarized. The data sets are compared, using a Helmholtz free energy formulation. Recommendations are given for which data sets are suited to serve as a basis for an equation of state formulation of the thermodynamic properties of {water+ammonia}. Gaps in the database are shown to give experimenters orientation for future research. © *1998 American Institute of Physics and American Chemical Society.* [S0047-2689(98)00301-8]

Key words: ammonia-water, data survey, mixture, thermodynamic properties.

Contents

List of Tables

List of Figures

[a]Author to whom correspondence should be addressed; Permanent address: Universität Hannover, Institut für Thermodynamik, Callinstrasse 36, 30167 Hannover, Germany.

Nomenclature

$\overline{A}$	molar Helmholtz free energy
c	coefficient
$\overline{C_p}$	molar isobaric heat capacity
$\overline{H}$	molar enthalpy
$\Delta\overline{H}$	molar enthalpy of mixing
N	number of tabulated data
p	pressure
R_m	universal gas constant
T	temperature
$\overline{V}$	molar volume
x	liquid mole fraction of ammonia
y	vapor mole fraction of ammonia
Φ	reduced Helmholtz free energy; $\overline{A}/R_mT$
δ	inverse reduced volume or reduced density; ϱ/ϱ_c
τ	inverse reduced temperature; T_c/T

Subscripts

c	critical
calc	calculated
exp	experimental
n	reducing property
tr	triple, solid-liquid-vapor boundary
01	pure component 1 (water)
02	pure component 2 (ammonia)

Superscripts

○	ideal gas
r	residual,
$'$	saturated liquid

1. Introduction

The mixture {water+ammonia} is of special interest as a working fluid in absorption cycles, refrigeration, and heat recovery. Recently, such mixtures have been proposed for use in the Kalina cycle for increased efficiency in power generation.[1] Water and ammonia are natural fluids which do not harm the environment. Therefore, they are also considered as alternative refrigerants to replace chlorofluorocarbons in some refrigeration applications.

From the thermodynamic point of view, water and ammonia are strongly polar substances. Their critical points are considerably different: critical temperatures differ by more than 240 K ($T_c=405.40$ K for ammonia and $T_c=647.096$ K for water). Also the critical pressure of water ($p_c=22.064$ MPa) is about twice as large as the critical pressure of ammonia ($p_c=11.339$ MPa). The normal boiling point of water (373.13 K) is about 135 K higher than the normal boiling point of ammonia (239.81 K). The mixture {water+ammonia} covers a very wide temperature range from below 200 K to 647.096 K. Compositional differences between the coexisting liquid and vapor phases are considerable. Mixing effects in liquid are particularly large. The liquid volume of mixing is in the order of -10% to -20% and the enthalpy of mixing is up to -4 kJ mol^{-1}.

The thermodynamic properties of the system {water+ammonia} have been measured by numerous researchers during the last 150 years. The vapor–liquid equilibrium (VLE) has been of primary interest due to the requirements of the absorption cycle. Further measurements deal with caloric or thermal behavior in the liquid and vapor phases.

Several data compilations have been published during the last 80 years.[2–10] However, none of them gives a complete overview and detailed comparisons of available experimental data necessary to establish an accurate equation of state.

To fill this gap, available measurements of the thermodynamic properties of {water+ammonia} mixtures have been compiled. Comparisons were conducted with an equation of state which was developed simultaneously with the data assessment by Tillner-Roth and Friend.[11] Based on this analysis, the most reliable measurements for the thermodynamic properties of {water+ammonia} are identified.

2. Survey of Experimental Data

Extensive experimental work has been carried out on the system {water+ammonia}. Available sources published through the end of 1995 are summarized in Table 1. Most references report vapor–liquid equilibrium (VLE) properties. Information on single-phase properties is more limited than available VLE data.

A significant effort has been made to survey and update old experimental data. Temperature conversion of measurements dated before 1927 into the current temperature scale (ITS-90) is not definitive because the first internationally accepted temperature scale was released that year. For older sources, temperatures were, therefore, assumed to be given according to IPTS-27. Although additional uncertainty occurs because of this assumption it is not regarded as a serious source of error, since the uncertainties of most older data are higher than those associated with any differences between the temperature scales.

A further difficulty arises when authors give their results in the form of smoothed tables or values rather than listing their original experimental data points. Furthermore, some of these smoothed sets of data are additionally based on measurements of other authors. Such sources are of limited value. Errors due to smoothing are already incorporated in the tabulated numbers. By including other experimental data during the smoothing procedure, the original experimental information is further obscured. Therefore, most of these results[2–6,53–56] were not further considered in the data comparisons.

Exceptions were made for the VLE data of Wucherer,[39] the saturated liquid enthalpies reported by Zinner[48], and the (p,T,x) data reported by Pierre.[21] Their tabulated values are based exclusively on their unreported measurements. The data of Zinner and of Pierre were only converted to ITS-90, and those of Wucherer were adjusted in this study. Wucherer reports vapor pressures for the pure components in addition to measurements for the mixtures. With these vapor pressures, saturation temperatures were calculated from the pure fluid equations of state.[57,58] These temperatures form a temperature scale for Wucherer's data and are used to correct the reported temperatures for the mixture measurements. The conversion process is described in the Appendix.

2.1. Vapor–Liquid Equilibrium

The distribution of VLE data is illustrated in a (T,x) diagram (Fig. 1) for the saturated liquid and in a (T,y) diagram, (Fig. 2) for the saturated vapor. Due to the large number of sources, only different types of VLE data are distinguished by different symbols, i.e., (p,T,x), (p,T,y), (p,T,x,y), and (T,x,y) data.

For the liquid side, a very large quantity of experimental data is available. The data extend to the critical line and reach down to the freezing line. However, two regions in the liquid become apparent where comparatively few data are available. The first region is observed between 250 K and 350 K for high ammonia concentrations. The second is the temperature range above 500 K at low and intermediate ammonia concentrations. Some data lying above the critical line drawn in Fig. 1 indicate experimental disagreement in the vicinity of the critical locus.

On the vapor side, the majority of measurements is found at high ammonia mole fractions. This is not surprising, because the vapor phase consists of almost pure ammonia over a large range of pressure and temperature. At lower ammonia concentrations, the number of experimental data becomes smaller.

In addition to data which are concerned with the (p,T,x,y) behavior, saturated liquid densities were reported for temperatures below 520 K. Additionally, the enthalpy of the saturated liquid has been reported by Zinner[48] up to 453 K. These data are discussed in the next section, together with caloric data in the single-phase region. For higher temperatures, no densities or caloric properties have been measured at saturated states. Most important, no information on saturated vapor densities or saturated vapor enthalpies could be found.

TABLE 1. Summary of experimental data for {water+ammonia}

Source	Year	N	Range of data		
			T/K	p/MPa	$x(NH_3)$
		(p,T,x) data (bubble-point measurements)[a]			
Carius[12]	1856	6	273–298	0.1	0.26–0.39
Foote[13]	1921	17	283–303	0.05–0.2	0.29–0.53
Gillespie *et al.*[14,15]	1985,1987	173	313–588	0.01–20.8	0.008–0.99
Guillevic *et al.*[16]	1985	13	403–503	1.3–7.1	0.07–0.7
Jennings[17]	1965	72	297–490	0.05–3.7	0.10–0.79
Mittasch *et al.*[18]	1926	51	273–334	0.01–0.9	0.21–0.52
Mollier[19]	1908	35	274–393	0.1–0.9	0.12–0.52
Perman[20]	1901	77	273–334	0.002–0.24	0.04–0.34
Pierre[a 21]	1959	(173)	233–513	0.004–4.8	0.05–0.41
Postma[22]	1920	202	196–480	0.001–17.8	0.127–1.0
Rizvi and Heidemann[23]	1987	36	304–618	0.02–21.9	0.007–0.88
Roscoe and Dittmar[24]	1859	34	273–327	0.002–0.26	0.07–0.69
Sassen *et al.*[25]	1990	111	389–613	1.3–21.5	0.189–0.8
Sims[26]	1861	16	273–373	0.002–0.28	0.06–0.52
		(p,T,y) data (dew-point measurements)[b]			
Guillevic *et al.*[16]	1985	21	403–503	0.8–6.7	0.195–0.974
Macriss *et al.*[6]	1964	16	333–390	1.5–3.6	>0.966
Neuhausen and Patrick[27]	1921	28	273–313	0.14–0.53	>0.972
Postma[22]	1920	17	433–508	10–16	0.74–0.932
Rizvi and Heidemann[23]	1987	11	345–618	0.9–19.3	0.08–0.993
Sassen *et al.*[25]	1990	133	373–453	0.1–9.7	0.2–0.9

TABLE 1. Summary of experimental data for {water+ammonia}—Continued

Source	Year	N	Range of data		
			T/K	p/MPa	$x(NH_3)$
		(p,T,x,y) data			
Clifford and Hunter[28]	1933	57	333–420	0.02–1.6	0.016–0.26
Gillespie *et al.*[14,15]	1985,1987	46	313–588	0.15–20.7	0.03–0.93
Guillevic *et al.*[16]	1985	5	403–503	4.4–5.7	0.09–0.64
Harms-Watzenberg[29]	1995	46	308–573	0.26–18.2	0.08–0.9
Hoshino *et al.*[30]	1975	21	240–363	0.101325	0.025–0.975
Inomata *et al.*[31]	1988	7	332	0.16–2.1	0.20–0.84
Iseli[e 32]	1985	44	354–493	3.6–16.1	0.47–0.89
Kurz[33]	1994	156	313–393	0.01–0.5	0.01–0.21
Müller *et al.*[34]	1988	40	373–473	0.19–3.1	0.04–0.32
Neuhausen and Patrick[27]	1921	31	273–313	0.1–0.5	0.25–0.66
Perman[35]	1903	42	273–333	0.002–0.08	0.03–0.23
Polak and Lu[36]	1975	23	363–420	0.1–0.44	0.001–0.04
Rizvi and Heidemann[23]	1987	285	303–618	0.03–22.5	0.01–0.99
Smolen *et al.*[c,d 37]	1991	198	293–413	0.01–3.1	0.04–0.96
Wilson[38]	1925	47	273–363	0.003–1.14	0.09–0.85
Wucherer[e 39]	1932	(432)	223–471	0.01–2	0.05–0.9
		(T,x,y) data			
Dvorak and Boublik[40]	1963	15	363.15	-	$x<0.03$, $y<0.3$
Hales and Drewes[41]	1979	30	276–297	-	$x<0.001$
Jones[42]	1963	18	420–600	-	$x<0.001$
		Partial pressures			
Hougen[43]	1925	9	287–300	-	0.01–0.18
		Saturated liquid densities			
Gillespie *et al.*[15]	1987	14	313–519	-	0.17–0.71
Harms-Watzenberg[f 29]	1995	60	243–413	-	0.1–0.9
Jennings[17]	1965	77	297–490	-	0.1–0.79
King *et al.*[44]	1930	28	293.15	-	0.005–0.98
Mittasch *et al.*[18]	1926	86	273–333	-	0.21–0.52
Wachsmuth[45]	1878	59	285	-	0.02–0.39
		$(p,\overline{V},T,x)$ data			
Carius[12]	1856	9	323–523	0.1	0.01–0.32
Ellerwald[46]	1981	323	323–523	0.04–8.3	0.08–0.97
Harms-Watzenberg[29] (liquid)	1995	1208	243–413	0.8–38	0.1–0.9
Harms-Watzenberg[29] (vapor)	1995	276	373–498	0.02–4.8	0.25–0.75
Neuhausen and Patrick[27]	1921	31	273–313	0.1–0.5	0.25–0.67
Staudt[47]	1984	175	298–403	2–20	0.1–0.9
		Saturated liquid enthalpy			
Zinner[a 48]	1934	(146)	203–453	-	0.1–0.9
		Enthalpy of mixing			
Baud and Gay[49]	1909	23	285	0.1	0.18–0.80
Staudt[47]	1984	92	298–373	5–12	0.09–0.93
		Enthalpy differences			
Macriss *et al.*[6]	1964	60	500–297	1.4–5.2	0.05–0.39
		Isobaric heat capacity			
Chan and Giauque[50]	1964	15	183–288	0.1	0.333
Hildenbrand and Giauque[51]	1953	60	197–290	0.1	0.5–0.67
Wrewsky and Kaigorodoff[52]	1924	23	275–334	0.1	0.01–0.40

[a]Smoothed data indicated with parentheses.
[b]Mole fractions in column 6 are vapor mole fractions.
[c]Vapor mole fractions are calculated.
[d]x and y are reported, but only total composition was measured.
[e]Constructed from smoothed data (see Appendix).
[f]Extrapolated.

2.2. Single-Phase Properties

Available sources of single-phase measurements are also listed in Table 1. $(p,\overline{V},T,x)$ data are plotted in a (p,T) diagram in Fig. 3. The extensive set of liquid densities of Harms–Watzenberg[29] covers temperatures between 243 K and 413 K up to 38 MPa for five different compositions. Additional $(p,\overline{V},T,x)$ measurements for the liquid density are reported by Staudt[47] (in terms of the volume of mixing), by Neuhausen and Patrick[27] and by Carius.[12] There are no single-phase liquid densities available above 413 K and below 243 K.

Two sources[29,46] report densities in the vapor phase reaching from 323 K to 523 K. They cover almost the entire concentration range. The maximum densities, however, do not exceed 1.5 mol/dm^3 and do not extend to the saturation

boundary. No vapor densities are available for higher and supercritical temperatures.

Measurements of caloric properties were found only for the liquid phase. Their distribution is shown in Fig. 4 in a (T,x) diagram. Enthalpies of mixing were measured by Staudt[47] in the liquid phase between 298 K and 373 K for pressures up to 12 MPa and also by Baud and Gay[49] at 285 K. Baud and Gay do not report pressures; therefore, atmospheric pressure conditions are assumed here. Macriss *et al.*[6] report experimental enthalpy differences in the liquid at starting temperatures up to 500 K and pressures up to 5 MPa. Measurements of the isobaric heat capacity are available from three sources[50–52] between 334 K and the freezing line. No pressures were given for these c_p values. It is assumed that these measurements were also carried out at atmospheric pressure conditions.

No caloric measurements could be found for the vapor or in the supercritical region.

2.3. Solid–Liquid-Vapor Boundary and Critical Locus

Temperatures of the solid–liquid-vapor locus are reported by five sources (Table 2). All sources are more than 70 years old. In addition, Postma[22] measured the triple-point pressure as a function of temperature. Measurements cover the entire concentration range from pure water to pure ammonia. Compositions and temperatures of the three eutectic points were only given by Postma[22] and by Rupert.[62]

A few values for temperature, pressure and composition of the critical line are reported by Rizvi and Heidemann,[23] Sassen *et al.*,[25] and by Postma.[22] The critical region and critical locus will be the topic of a separate paper by Rainwater and Tillner-Roth.[63]

3. Data Comparisons

3.1. The Triple-Point Line

The triple-point line is shown in a (T,x) diagram [Fig. 5(a)]. Three eutectic points are observed near $x=0.334$, $x=0.584$, and $x=0.815$. Two temperature maxima occur at the compositions of the solid compounds $NH_3 \cdot H_2O$ ($x=0.5$) and $2NH_3 \cdot H_2O$ ($x=2/3$). The temperature of the solid-liquid-vapor boundary has been correlated by the following four equations:

$$0 \leqslant x \leqslant 0.33367: \frac{T_{tr}(x)}{273.16\ \mathrm{K}} - 1 = c_{11}x + c_{12}x^2 + c_{13}x^7$$

$$0.33367 < x \leqslant 0.58396: \frac{T_{tr}(x)}{193.549\ \mathrm{K}} - 1 = c_{21}(x-0.5)^2$$

$$0.58396 < x \leqslant 0.81473: \frac{T_{tr}(x)}{194.380\ \mathrm{K}} - 1 = c_{31}(x-2/3)^2 + c_{32}(x-2/3)^3$$

$$0.81473 < x \leqslant 1: \frac{T_{tr}(x)}{195.495\ \mathrm{K}} - 1 = c_{41}(1-x) + c_{42}(1-x)^4. \quad (1)$$

The coefficients are

$$c_{11} = -0.343\,9823 \quad c_{12} = -1.327\,4271$$
$$c_{13} = -274.973 \quad c_{21} = -4.987\,368$$
$$c_{31} = -4.886\,151 \quad c_{32} = +10.372\,98$$
$$c_{41} = -0.323\,998 \quad c_{42} = -15.875\,60.$$

Deviations of measured triple-point temperatures from calculated values are shown in Fig. 5(b). The measurements of Postma,[22] Elliot,[60] and of Rupert[62] generally agree within ± 1 K and are represented by Eq. (1) within the same limits of uncertainty. The results of Baume and Tykociner[59] show systematic deviations up to $+10$ K at low ammonia concentrations. Deviations of triple-point temperatures measured by Pickering[61] in 1891 reach up to $+8$ K. In the vicinity of the first eutectic point near $x=0.334$, the different data sets disagree considerably. The reported eutectic temperatures vary between 153 K from Ref. 62 and 173 K from Ref. 22. Deviations from Eq. (1) in this concentration range are, therefore, greater than for the rest of the triple-point line. For the other eutectics, temperatures agree within ± 0.2 K and compositions within ± 0.01 mole fraction of ammonia.

It is concluded that the most reliable data are those of Postma,[22] Elliott,[60] and Rupert[62] because they show the best agreement. Those of Baume and Tykociner[59] and of Pickering[61] seem to be of lesser accuracy. No comparisons are given for the triple-point pressure, because only one data source is available (Postma[22]).

3.2. Fluid Properties

Experimental data in the fluid region of {water+ammonia} are compared with the help of a fundamental equation of state. This equation was established simultaneously with the data survey and is described in detail by Tillner-Roth and Friend.[11] It is written in terms of the reduced Helmholtz free energy according to

$$\frac{\overline{A}}{R_m T} = \Phi = \Phi^\circ(\tau^\circ, \delta^\circ, x) + \Phi^r(\tau, \delta, x). \quad (2)$$

The ideal part Φ°, depending on the dimensionless variables $\tau^\circ = T_n^\circ/T$, $\delta^\circ = \overline{V_n^\circ}/\overline{V}$, and mole fraction x of ammonia describes the ideal gas properties of the mixture. The residual part Φ^r, depending on $\tau = T_n(x)/T$, $\delta = \overline{V_n}(x)/\overline{V}$, and x, acts as a correction term for the ideal gas with respect to the real mixture. The dimensionless variables τ and δ of the residual part depend on the composition of the mixture. The model is based on accurate equations of state for the pure components

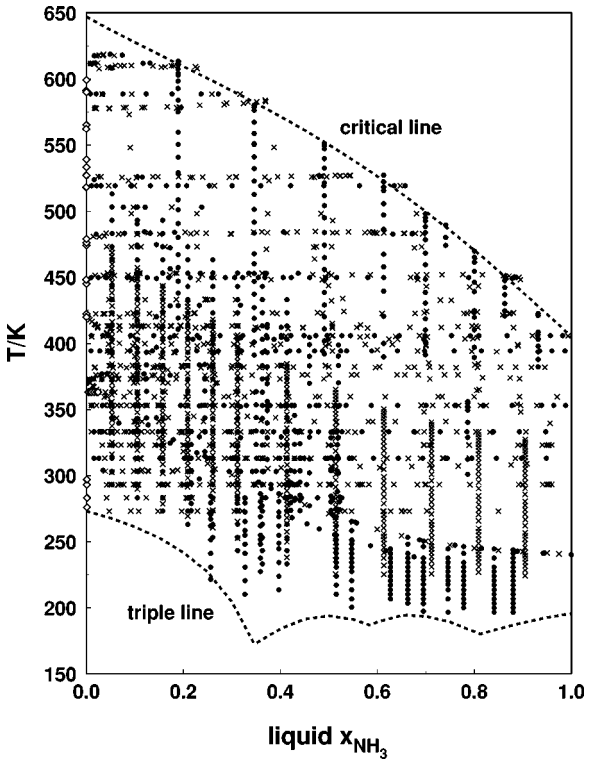

FIG. 1. Distribution of measured (p,T,x) data (●), (p,T,x,y) data (×), and (T,x,y) data (◇) in a T,x diagram.

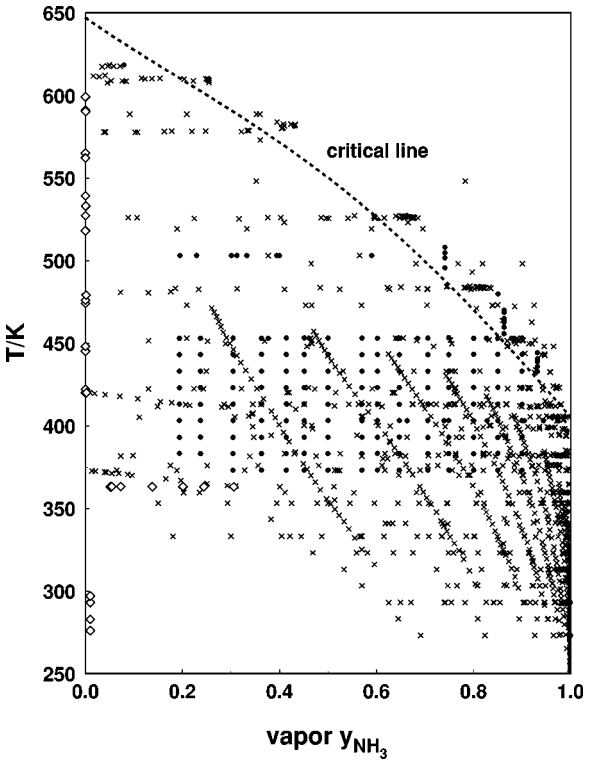

FIG. 2. Distribution of measured (p,T,y) data (●), (p,T,x,y) data (×), and (T,x,y) data (◇) in a T,y diagram.

developed by Pruss and Wagner[57] for water and by Tillner-Roth *et al.*[58] for ammonia. All thermodynamic properties can be calculated from this fundamental equation of state. It is valid between the triple-point line and the critical locus as well as for the single-phase liquid and vapor regions for all compositions. A detailed description of the fundamental equation of state is given by Tillner-Roth and Friend.[11]

3.2.1. VLE Data

Comparisons for (p,T,x), (p,T,y), and (p,T,x,y) data are given in Figs. 6–8. Figures 6 and 7 show deviations of measured vapor and liquid mole fractions, y and x, of ammonia from those obtained from calculations using Eq. (2). The measured pressures and temperatures were used as input values. Vapor mole fractions compared in Fig. 8 were calculated for given T and x.

Due to the large number of sources, it was decided to discuss all data sets separately. It is not the intention of this work to evaluate the accuracy of the underlying equation of state. Deviations between data and the equation of state, however, may sometimes indicate an inconsistency between different sets of data. Subsequently, all sources are discussed in alphabetical order. Their large number made it necessary to split Figs. 6 and 7 into 6(a)–6(f) and into 7(a)–7(e). Experimental data which overlap are combined so that each diagram represents the situation in a limited region.

• **Carius (1856),[12] [Fig. 6(a)]**

Six (p,T,x) data were reported in this early work. The liquid mole fractions show systematic deviations of about -0.03 from other more reliable data.

• **Clifford and Hunter (1933),[28] [Figs. 6(d), 7(a)]**

This set of (p,T,x,y) data covers temperatures between 333 K and 420 K at low liquid ammonia concentrations. Liquid mole fractions agree within ± 0.01 with data from Perman,[35] Mollier,[19] and Pierre[21] at low temperatures. The scatter increases slightly at higher temperatures but remains within ± 0.02. Vapor mole fractions show a large scatter up to ± 0.06. Overall, the accuracy of this data set is lower than that of other data.

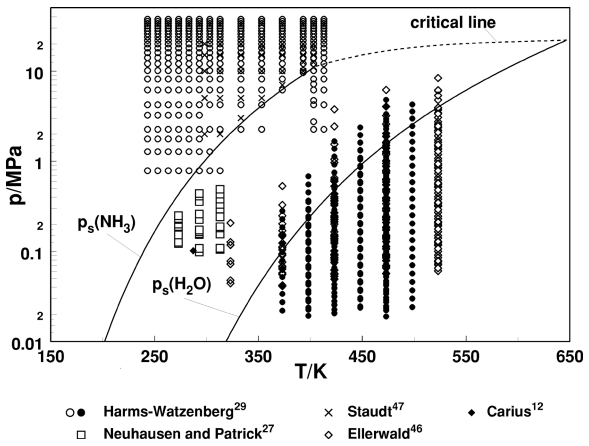

FIG. 3. Distribution of measured $(p,\overline{V},T,x)$ data in a p,T diagram.

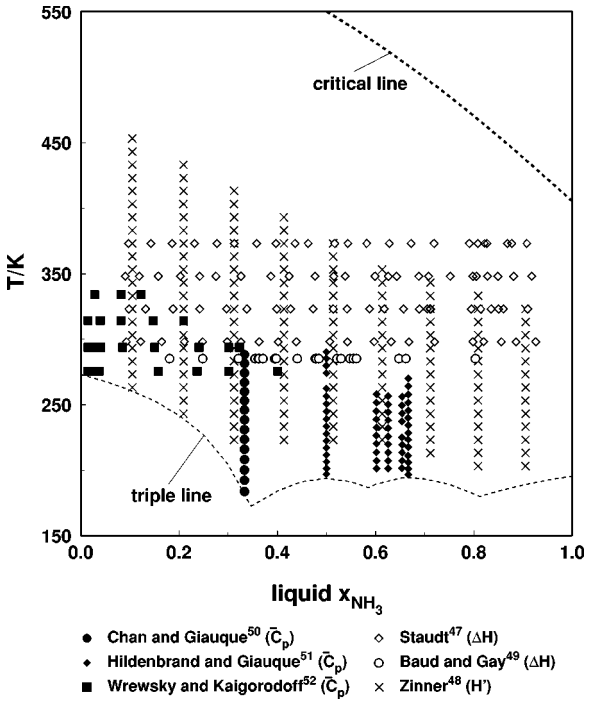

FIG. 4. Distribution of liquid caloric data in a T,x diagram.

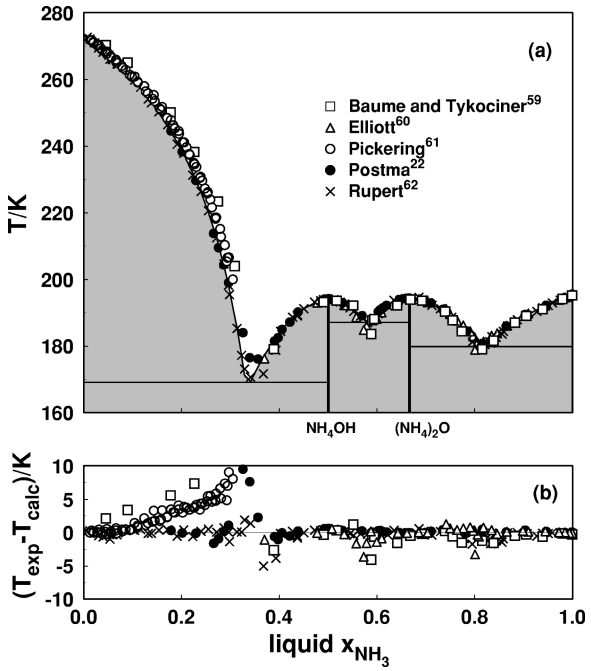

FIG. 5. Triple-point temperatures of {water+ammonia}. Triple-point temperatures T_{calc} in (b) are calculated from Eq. (1).

• Dvorak and Boublik (1963),[40] [Fig. 8]

Dvorak and Boublik report some (T,x,y) values at very low ammonia concentrations. Vapor compositions agree within the experimental scatter with the overlapping data of Polak and Lu.[36] They are regarded as being sufficiently reliable to be used to establish an accurate equation of state.

• Foote (1921),[13] [Fig. 6(a)]

Foote reports (p,T,x) data at two temperatures (283 K and 303 K). These liquid compositions agree generally with the data of Neuhausen and Patrick[27] but overlap more reliable data.

• Gillespie *et al.* (1985, 1987),[14,15] [Figs. 6(c), 7(c), 7(d)]

Both references report results from the same experimental study. However, the values from Ref. 15 are slightly different than the values listed in Ref. 14. Differences are found in the values for pressures and compositions. Generally, these corrections are small, but the values from Ref. 15 seem to be slightly more consistent and should, therefore, be preferred; data from Ref. 14 are not shown in the figures.

TABLE 2. Summary of experimental data for the triple-point line of {water+ammonia}

Source	Year	N	Composition range $x(NH_3)$
Triple-point temperatures			
Baume and Tykociner[59]	1914	13	0.04–0.58
Elliot[60]	1924	35	0.37–1.0
Postma[22]	1920	39	0.04–1.0
Pickering[61]	1891	67	0.01–0.31
Rupert[62]	1910	86	0.007–0.99
Triple-point pressures			
Postma[22]	1920	48	0.04–1.0

(p,T,x,y) data and (p,T,x) data reported here cover a wide range of composition and temperature. Liquid mole fractions are internally consistent within ± 0.03 and agree well with the results of Sassen *et al.*[25] and of Iseli[32] at high temperatures. Vapor mole fractions also scatter by ± 0.03 except at lower temperatures, where the measured vapor composition seems to be more accurate. Vapor mole fractions at high y values agree well with the results of Macriss *et al.*,[6] but are about 0.01 lower than results of Iseli[32] and other sources.

Generally, the results of Gillespie *et al.* show a larger scatter than other reliable data. However, since they cover a wide range of temperature and composition they are useful to establish a reliable equation of state.

• Guillevic *et al.* (1985),[16] [Figs. 6(c), 7(a)]

13 (p,T,x), 5 (p,T,x,y), and 21 (p,T,y) data are reported between 400 K and 500 K in a wide concentration range. Liquid and vapor mole fractions show systematic deviations up to ± 0.05. Because of the large deviations, these data may not be adequate for correlation purposes.

• Hales and Drewes (1979),[41] [Fig. 8]

(T,x,y) values are reported for very dilute ammonia solutions between 270 K and 300 K. No other data are available in this range for comparisons. Due to the lack of other sets of data in this region, no recommendation can be given for this data set, although large systematic deviations are observed between the data and Eq. (2).

• Harms-Watzenberg (1995),[29] [Figs. 6(c), 7(b)]

46 (p,T,x,y) data are reported covering a wide range of composition and temperature. Liquid mole fractions show a scatter up to 0.04; those of the vapor show systematic devia-

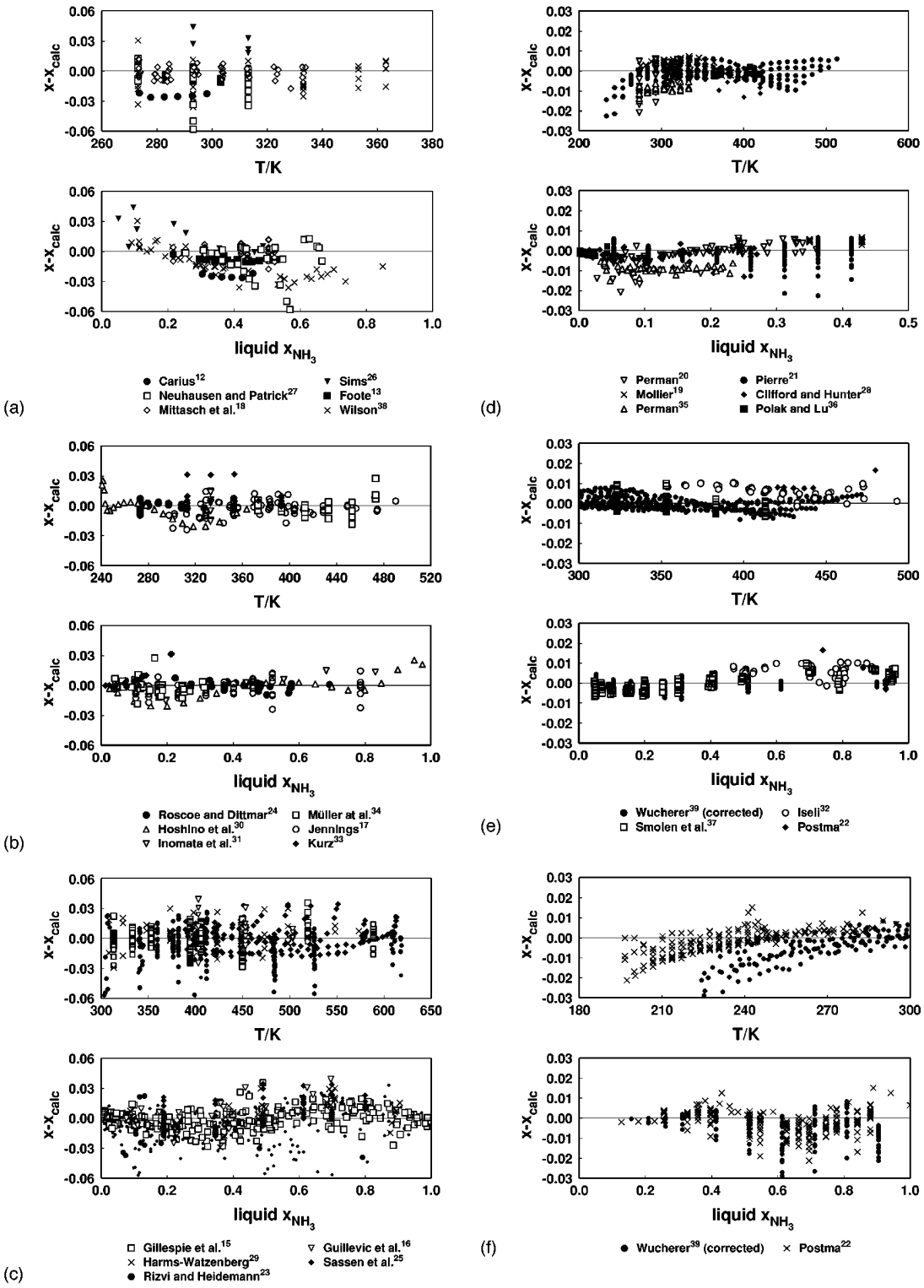

FIG. 6. (a)–(f) Deviations between measured liquid mole fractions x and values calculated from Eq. (2) at tabulated values of pressure p and temperature T.

tions from other reliable data up to ± 0.10. Data of higher quality are available to establish an equation of state.

• **Hoshino** *et al.* **(1975),[30] [Figs. 6(b), 7(a)]**

21 (p,T,x,y) data are reported at atmospheric pressure covering the whole concentration range. Liquid mole fractions show systematic deviations from other reliable data up to ± 0.03. Vapor mole fractions are about 0.02 lower than those from other sources. Data[22] which are more reliable overlap the results of Hoshino *et al.*

• **Hougen (1925)[43]**

Hougen reports nine ammonia partial pressures in the vapor for low liquid mole fractions and temperatures between

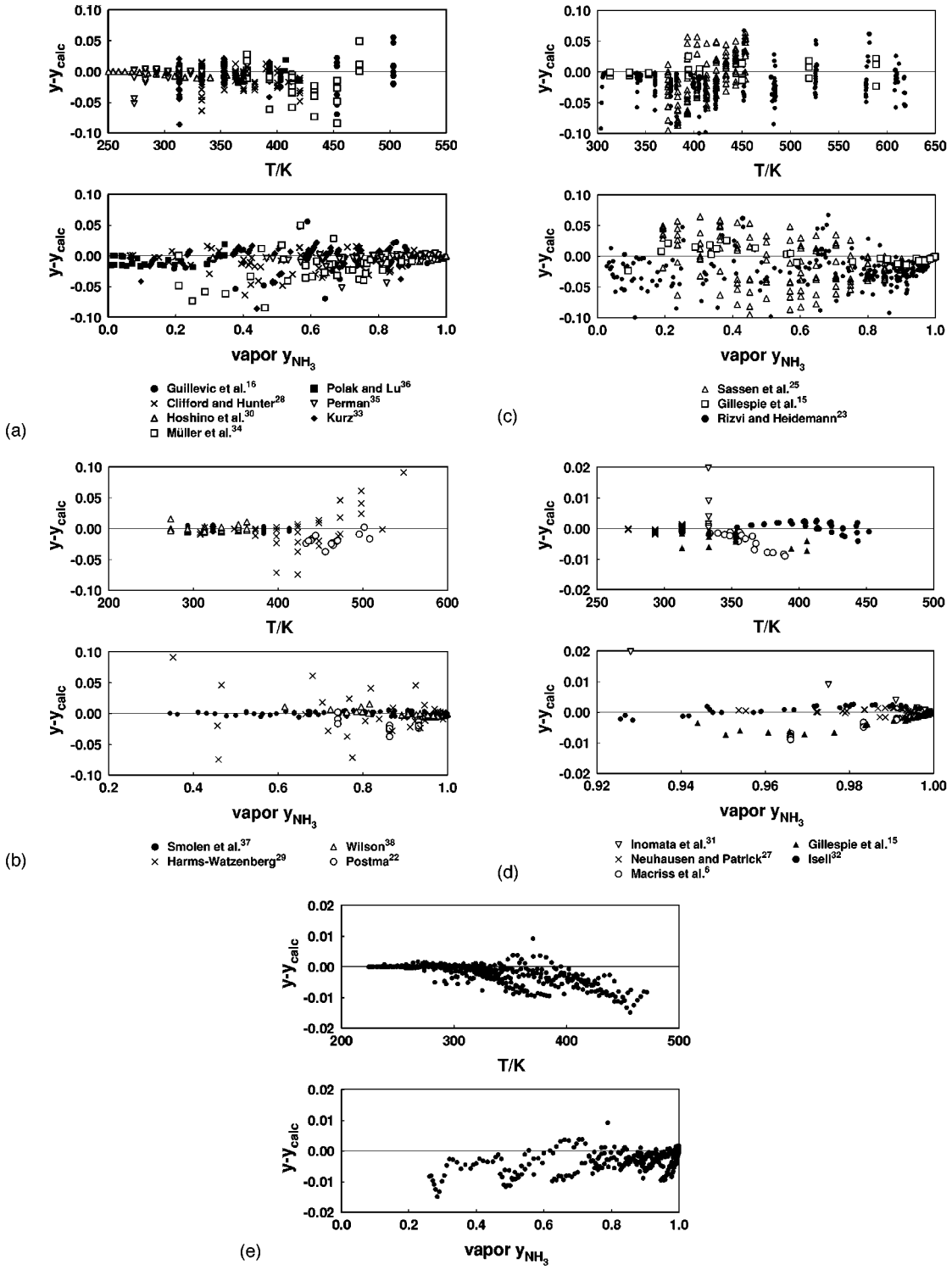

FIG. 7. (a)–(d) Deviations between measured vapor mole fractions y and values calculated from Eq. (2) at tabulated values of pressure p and temperature T. (e) Deviations between Wucherer's corrected vapor mole fractions y from Table 3 and values calculated from Eq. (2) at tabulated values of pressure p and temperature T.

287 K and 300 K. Since he does not report a total pressure or the corresponding water partial pressures these measurements are incomplete compared to other VLE measurements. In addition they completely overlap other results and therefore will not be considered further.

• **Inomata *et al.* (1988),[31] [Figs. 6(b), 7(d)]**

Seven (p,T,x,y) data are reported at 332 K. Liquid and vapor mole fractions show systematic deviations up to 0.02 and, therefore, are not adequate to establish an equation of state.

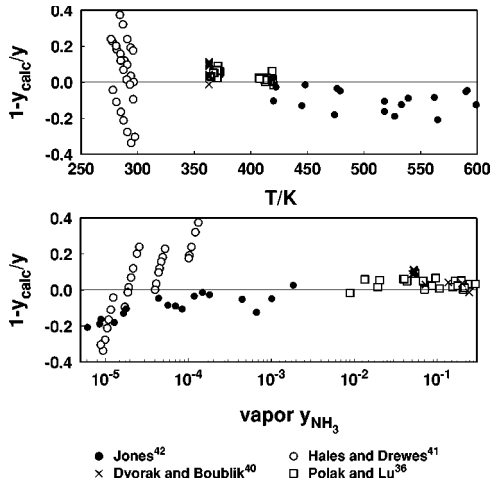

FIG. 8. Relative deviations of vapor mole fractions y from values calculated from Eq. (2) at tabulated values of temperature T and vapor mole fraction y.

• Iseli (1985),[32] [Figs. 6(e), 7(d)]

Iseli measured 44 (p,T,x,y) data at fairly high pressures, temperatures and ammonia concentrations. Liquid mole fractions agree very well within ± 0.01 with the results of Gillespie *et al.*[14,15] and Sassen *et al.*[25] They are about 0.005–0.01 higher than the results of Smolen *et al.*[37] Vapor mole fractions agree with other data within ± 0.01. These data are recommended to establish an equation of state.

• Jennings (1965),[17] [Fig. 6(b)]

72 (p,T,x) data are reported by Jennings between 297 K and 490 K. The liquid mole fractions scatter within ± 0.02 but generally agree with other reliable data. There are data of better quality which overlap Jennings' results.

• Jones (1963),[42] (Fig. 8)

Liquid mole fractions of these (T,x,y) data extend to lower values than those of Dvorak and Boublik.[40] The results of Jones also cover a wide temperature range. In the overlapping region, they agree well with results from Dvorak and Boublik. Although a slight systematic deviation between the data and Eq. (2) is observed, they are also deemed appropriate to support an equation of state at low ammonia concentrations.

• Kurz (1994),[33] [Figs. 6(b), 7(a)]

156 (p,T,x,y) data were measured at liquid mole fractions below 0.21. The large number of data is due to extensive replicate measurements. If the results had been averaged, the total number of points would be close to 30. Liquid mole fractions are very reliable, showing deviations within ± 0.01 or better. Exceptions are measurements at liquid mole fractions near 0.2 where deviations increase up to 0.03. The scatter of vapor mole fractions is larger, within ± 0.02 with a few exceptions at low temperatures where deviations are up to 0.08. Due to the deviations for the vapor mole fractions, these data seem questionable when establishing a reliable equation of state. The liquid mole fractions, however, seem to be relatively reliable.

• Macriss *et al.* (1964),[6] [Fig. 7(d)]

Macriss and his co-workers report 16 (p,T,y) data at very high ammonia concentrations. Vapor mole fractions are about 0.01 lower than most from other sources, except those measured by Gillespie *et al.*[14,15] It is unclear which behavior is the more reliable, but because the equation used for the comparisons is also fitted to $(p,\overline{V},T)$ data in the superheated vapor region, this deviation suggests an inconsistency between vapor mole fractions of Gillespie *et al.*[15] and Macriss *et al.*[6] and vapor densities measured by Harms-Watzenberg[29] or Ellerwald,[46] for example. Further measurements, not only of vapor composition, but also of thermal and caloric properties in the vapor, are needed to resolve this systematic difference.

• Mittasch *et al.* (1926),[18] [Fig. 6(a)]

51 (p,T,x) data between 273 K and 334 K are reported. Liquid mole fractions generally agree with other reliable data within ± 0.02. However, they need not be incorporated in the development of a thermodynamic surface because they overlap data of better quality.

• Mollier (1908),[19] [Fig. 6(d)]

35 (p,T,x) data are reported by Mollier. The liquid mole fractions agree with those of Perman[35] within ± 0.005 and also show excellent agreement with data from other reliable sources. Although these data are old, they are of high accuracy.

• Müller *et al.* (1988),[34] [Figs. 6(b), 7(a)]

40 (p,T,x,y) data are reported at low ammonia concentrations between 373 K and 473 K. In general, liquid mole fractions agree with other reliable data, but show a scatter up to ± 0.03. Vapor mole fractions are evidently of poorer quality showing systematic deviations of up to ± 0.08. More accurate data are available for correlation purposes.

• Neuhausen and Patrick (1921),[27] [Figs. 6(a), 7(d)]

31 (p,T,x,y) data and 28 (p,T,y) data are reported between 273 K and 313 K at intermediate liquid compositions. Liquid mole fractions show a large scatter up to 0.06 and deviate systematically from other data. Mole fractions in the vapor are above 0.95 in this temperature range. Due to the high ammonia concentrations the scatter is small. However, some vapor mole fractions of Neuhausen and Patrick show systematic deviations from other reliable data around $y = 0.99$.

• Perman (1901)[20] and (1903),[35] [Figs. 6(d), 7(a)]

The first set of measurements reported by Perman[20] comprises 77 (p,T,x) data at low ammonia concentrations. The scatter of liquid mole fractions is well within ± 0.01. Liquid mole fractions from Perman's (p,T,x,y) data published two years later, however, show a systematic offset of -0.01 compared to other sources. The vapor mole fractions from the second set agree within ± 0.01 with other reliable data, especially at intermediate compositions. However, they show an increasing deviation with decreasing temperatures. The first series of Perman[20] (1901) is recommended while the second set (Perman[35]) may have slight systematic errors.

• Pierre (1959),[21] [Fig. 6(d)]

Pierre published a table of smoothed (p,T,x) data based on unreported measurements. These smoothed data were transformed into the new temperature scale (ITS-90) and

used in the comparisons. Liquid mole fractions agree within ± 0.01 with other measurements. The downturn at low temperatures is slightly sharper than that observed for Postma's[22] data, [Fig. 6(f)]. Pierre's data are useful to establish an equation of state, but original measurements, as those of Postma,[22] should be preferred.

• Polak and Lu (1975),[36] [Figs. 6(d), 7(a), 8]

23 (p,T,x,y) data were measured at low ammonia concentrations $x<0.04$. Naturally, the scatter in x is smaller than for data at higher mole fractions; the scatter is generally below 0.005. Vapor mole fractions agree very well with results of Dvorak and Boublik[40] These data are recommended to establish an equation of state in order to obtain a good fit at low ammonia concentrations.

• Postma (1920),[22] [Figs. 6(e), 6(f), 7(b)]

202 (p,T,x) and 17 (p,T,y) data are reported in this reference. The (p,T,x) data mainly cover subatmospheric pressures and extend down to the triple-point line. (p,T,y) data and some (p,T,x) data were measured at high pressures and temperatures close to the critical line. Beside this series, no other VLE data are available below 230 K to compare with. At temperatures between 230 K and 280 K, the liquid mole fractions agree within ± 0.01 with the results of Perman[35] and Mollier,[19] and smoothly connect to the data measured by Smolen *et al.*[37] Liquid mole fractions are about 0.01–0.02 higher than those of the corrected data of Wucherer[39] described below. At temperatures below 230 K, the scatter becomes larger due to the higher sensitivity of liquid mole fractions to uncertainties in pressure.

Liquid compositions of near-critical data agree well with other data. Deviations are ± 0.02 which is small when considering that mole fractions have a high uncertainty in this region. Vapor mole fractions show deviations within ± 0.03.

The (p,T,x) data of Postma at low temperatures are regarded as reliable and can be used to establish an equation of state, especially because it is the only set of data currently available down to the triple-point line. Also some of the (p,T,x) data and (p,T,y) data at near-critical temperatures seem to be useful. For low temperatures, further experimental VLE data would be desirable to validate Postma's results.

• Rizvi and Heidemann (1987),[23] [Figs. 6(c), 7(c)]

Rizvi and Heidemann report one of the most extensive sets

TABLE 3. Corrected VLE data of Wucherer[a]

p/kPa	T/K	y	T/K	y	T/K	y	T/K	y	T/K	y
	$x=0.0527$		$x=0.1052$		$x=0.1573$		$x=0.2091$		$x=0.2607$	
10.132	302.60		289.78		278.86		269.24		260.62	
20.265	316.08	0.596	303.46	0.808	293.04	0.903	282.92	0.953	273.71	0.980
30.398	325.13	0.570	312.31	0.791	301.79	0.893	291.47	0.946	282.15	0.976
40.530	332.20	0.555	319.28	0.780	308.56	0.886	298.14	0.940	288.72	0.973
50.662	337.58	0.543	324.57	0.770	313.66	0.878	303.15	0.936	293.64	0.969
60.795	342.00	0.533	328.89	0.760	317.88	0.872	307.47	0.933	297.77	0.966
70.928	345.92	0.523	332.72	0.752	321.62	0.867	311.11	0.929	301.41	0.964
81.060	349.58	0.514	336.28	0.745	324.97	0.861	314.37	0.925	304.66	0.962
91.192	352.79	0.505	339.38	0.739	328.08	0.856	317.37	0.922	307.76	0.959
101.33	355.91	0.497	342.40	0.733	331.09	0.851	320.18	0.920	310.57	0.957
121.59	361.20	0.484	347.78	0.723	336.17	0.845	325.15	0.915	315.34	0.955
141.86	365.92	0.474	352.40	0.713	340.49	0.839	329.48	0.911	319.56	0.951
162.12	370.04	0.465	356.42	0.704	344.31	0.832	333.30	0.905	323.09	0.947
182.39	373.66	0.457	359.95	0.696	347.73	0.826	336.72	0.900	326.51	0.944
202.65	376.96	0.449	363.15	0.689	350.93	0.821	339.82	0.895	329.61	0.942
253.31	384.28	0.433	370.47	0.674	358.15	0.809	346.94	0.888	336.52	0.936
303.98	390.51	0.420	376.60	0.661	363.98	0.798	352.67	0.880	342.25	0.932
354.64	395.95	0.409	381.94	0.649	370.22	0.789	357.70	0.872	347.19	0.926
405.30	400.72	0.399	386.70	0.637	373.99	0.779	362.27	0.866	351.75	0.921
455.96	405.03	0.391	390.92	0.627	378.21	0.771	366.40	0.860	355.80	0.916
506.63	408.97	0.383	394.96	0.618	382.06	0.763	370.35	0.854	359.45	0.913
607.95	416.28	0.367	402.16	0.600	389.25	0.749	377.24	0.843	366.32	0.904
709.28	422.51	0.354	408.50	0.583	395.39	0.735	383.07	0.832	372.16	0.896
810.60	428.29	0.342	414.17	0.569	400.86	0.722	388.54	0.823	377.43	0.889
911.93	433.54	0.330	419.22	0.556	405.80	0.712	393.59	0.815	382.07	0.882
1013.3	438.28	0.320	423.86	0.544	410.34	0.700	398.21	0.807	386.49	0.875
1114.6	442.48	0.312	428.06	0.534	414.54	0.691	402.42	0.799	390.60	0.870
1215.9	446.28	0.305	432.07	0.524	418.45	0.682	406.23	0.792	394.31	0.866
1317.2	449.94	0.298	435.82	0.515	422.20	0.674	409.78	0.786	397.96	0.860
1418.6	453.38	0.290	439.36	0.507	425.74	0.666	413.12	0.779	401.20	0.855
1519.9	456.64	0.284	442.53	0.500	429.01	0.658	416.29	0.772	404.28	0.850
1621.2	459.93	0.279	445.71	0.493	432.29	0.651	419.47	0.766	407.35	0.846
1722.5	462.98	0.275	448.67	0.487	435.35	0.644	422.33	0.760	410.22	0.841
1823.9	465.90	0.271	451.58	0.481	438.17	0.637	425.15	0.756	412.94	0.836
1925.2	468.79	0.266	454.47	0.476	440.95	0.631	427.83	0.750	415.62	0.831
2026.5	471.47	0.261	457.15	0.471	443.54	0.625	430.32	0.744	418.00	0.827

TABLE 3. Corrected VLE data of Wucherer[a]—Continued

p/kPa	T/K	y	T/K	y	T/K	y	T/K	y	T/K	y
	$x=0.3119$		$x=0.4136$		$x=0.5141$		$x=0.6134$		$x=0.7117$	
10.132	252.60		238.27	1.000	225.43	1.000				
20.265	265.19	0.992	249.86	0.999	236.32	1.000	225.29	1.000		
30.398	273.43	0.991	257.59	0.999	243.55	1.000	232.11	1.000	225.57	1.000
40.530	279.80	0.988	263.66	0.999	249.22	1.000	237.58	1.000	231.04	1.000
50.662	284.83	0.986	268.10	0.999	253.58	1.000	241.76	1.000	235.23	1.000
60.795	288.86	0.984	272.04	0.998	257.21	0.999	245.49	1.000	238.68	1.000
70.928	292.30	0.982	275.40	0.998	260.39	0.999	248.68	1.000	241.67	1.000
81.060	295.55	0.981	278.44	0.997	263.23	0.999	251.52	1.000	244.31	1.000
91.192	298.55	0.980	281.24	0.997	265.92	0.999	253.91	1.000	246.89	1.000
101.33	301.36	0.979	283.94	0.996	268.42	0.999	256.10	1.000	249.18	1.000
121.59	306.02	0.977	288.40	0.996	272.67	0.999	260.34	1.000	253.11	1.000
141.86	310.15	0.975	292.22	0.995	276.39	0.999	264.16	1.000	256.83	1.000
162.12	313.78	0.973	295.66	0.994	279.73	0.999	267.51	1.000	259.99	1.000
182.39	317.00	0.972	298.77	0.993	282.65	0.999	270.32	1.000	262.80	1.000
202.65	319.89	0.970	301.67	0.992	285.34	0.999	272.91	1.000	265.28	1.000
253.31	326.71	0.966	308.08	0.991	291.45	0.999	278.93	1.000	270.90	1.000
303.98	332.14	0.961	313.41	0.990	296.49	0.998	283.86	0.999	275.83	1.000
354.64	337.07	0.957	318.04	0.988	301.01	0.998	288.27	0.999	280.04	1.000
405.30	341.44	0.955	322.21	0.986	305.08	0.997	292.34	0.999	283.91	1.000
455.96	345.39	0.952	325.97	0.984	308.85	0.997	295.94	0.999	287.32	1.000
506.63	349.14	0.949	329.33	0.983	312.32	0.996	299.10	0.999	290.39	1.000
607.95	355.51	0.943	335.78	0.979	318.45	0.994	304.73	0.999	296.10	1.000
709.28	361.24	0.937	341.21	0.976	323.59	0.992	309.86	0.998	301.03	0.999
810.60	366.41	0.932	346.18	0.973	328.25	0.991	314.52	0.997	305.49	0.999
911.93	371.05	0.927	350.71	0.971	332.58	0.990	318.64	0.996	309.50	0.999
1013.3	375.37	0.921	354.93	0.968	336.49	0.988	322.34	0.995	313.30	0.998
1114.6	379.38	0.916	358.74	0.965	340.10	0.986	325.86	0.994	316.72	0.998
1215.9	383.09	0.913	362.25	0.962	343.52	0.985	329.18	0.993	320.04	0.998
1317.2	386.55	0.908	365.51	0.959	346.77	0.983	332.43	0.993	322.99	0.998
1418.6	389.77	0.904	368.73	0.957	349.69	0.982	335.44	0.992	325.80	0.997
1519.9	392.86	0.900	371.63	0.955	352.49	0.981	338.26	0.992	328.52	0.997
1621.2	395.93	0.897	374.49	0.954	355.25	0.979	340.91	0.991	331.17	0.997
1722.5	397.80	0.894	377.17	0.952	357.84	0.978	343.40	0.991	333.57	0.996
1823.9	401.42	0.891	379.69	0.950	360.36	0.978	345.73	0.991	335.90	0.996
1925.2	404.40	0.887	382.16	0.948	362.83	0.977	348.09	0.991	338.25	0.995
2026.5	406.18	0.884	384.64	0.946	365.00	0.976	350.26	0.990	340.32	0.995
	$x=0.8088$		$x=0.9049$				$x=0.8088$		$x=0.9049$	
40.530	226.80	1.000	224.36	1.000	506.63		284.58	1.000	280.37	1.000
50.662	231.11	1.000	228.39	1.000	607.95		290.17	1.000	285.64	1.000
60.795	234.56	1.000	231.64	1.000	709.28		294.90	1.000	290.37	1.000
70.928	237.47	1.000	234.46	1.000	810.60		299.16	1.000	294.53	1.000
81.060	240.09	1.000	237.08	1.000	911.92		303.06	1.000	298.33	1.000
91.192	242.58	1.000	239.46	1.000	1013.3		306.66	0.999	301.92	1.000
101.33	244.76	1.000	241.64	1.000	1114.6		310.08	0.999	305.15	1.000
121.59	248.68	1.000	245.45	1.000	1215.9		313.21	0.999	308.17	1.000
141.86	252.00	1.000	248.68	1.000	1317.2		316.15	0.999	311.11	1.000
162.12	254.97	1.000	251.65	1.000	1418.6		318.85	0.999	313.71	1.000
182.39	257.67	1.000	254.35	1.000	1519.9		321.39	0.999	316.25	1.000
202.65	260.06	1.000	256.73	1.000	1621.2		323.83	0.999	318.69	1.000
253.31	265.77	1.000	262.14	1.000	1722.5		326.24	0.998	321.01	1.000
303.98	270.41	1.000	266.68	1.000	1823.9		328.57	0.998	323.23	0.999
354.64	274.06	1.000	270.57	1.000	1925.2		330.92	0.998	325.38	0.999
405.30	278.28	1.000	274.25	1.000	2026.5		333.08	0.998	327.35	0.999
455.96	281.60	1.000	277.48	1.000						

[a]See Ref. 39.

of VLE data. A total of 332 (p,T,x), (p,T,x,y), and (p,T,y) data cover the entire concentration range between 303 K and the critical line. The accuracy of all data, however, generally seems to be poor. Liquid and vapor mole fractions show large scatter, sometimes exceeding the limits of Figs. 6(c) and 7(c), which are ± 0.10. Liquid mole fractions seem to be about 0.02–0.03 lower than other reliable data. The deviations are worst at 482 K and 525 K, while the scatter is smaller at lower temperatures. It is unfortunate that this comprehensive work has such large uncertainties.

• **Roscoe and Dittmar (1859),[24] [Fig. 6(b)]**

(p,T,x) data of good accuracy are reported by Roscoe and Dittmar. Their liquid mole fractions agree within ± 0.01 with other reliable data. Slightly higher deviations occur at low ammonia concentrations.

• **Sassen *et al.* (1990),[25] [Figs. 6(c), 7(c)]**

Two extensive sets of (p,T,x) and (p,T,y) data are reported by Sassen *et al.* The bubble-point measurements cover high temperatures and pressures over the whole concentration range reaching up to the critical line. The dew-point measurements are restricted to pressures below 10 MPa. Liquid mole fractions agree within ± 0.015 with data from Gillespie *et al.*,[14,15] even very close to the critical locus. Small systematic deviations are observed between measurements carried out at different compositions. In sharp contrast, the dew-point measurements show a large scatter up to ± 0.10 in y. While the bubble-point measurements are very useful to establish an equation of state, the dew-point measurements may not be sufficiently reliable.

• **Sims (1861),[26] [Fig. 6(a)]**

Sims reports 16 (p,T,x) values. Liquid mole fractions show large deviations up to 0.05 from most other data. These data are, therefore, of lesser importance.

• **Smolen *et al.* (1991),[37] [Figs. 6(e), 7(b)]**

A large set of (p,T,x,y) data is reported by Smolen *et al.* covering the whole concentration range between 293 K and 413 K. Originally, total composition was measured. Liquid and vapor compositions were determined using an equation of state. Liquid mole fractions are internally consistent with respect to temperature and composition. They agree within ± 0.01 with other reliable data. Also vapor compositions show a high degree of internal consistency as expected, since they were derived from an equation of state. Overall, this data set is useful to establish an equation of state.

• **Wilson (1925),[38] [Figs. 6(a), 7(b)]**

The liquid mole fractions of the 47 (p,T,x,y) data reported by Wilson show systematic deviations up to 0.03 from other sets of data. The vapor mole fractions seem to be of better quality and agree with other measurements within ± 0.02. Due to the large deviations on the bubble curve, this data set is not recommended as a basis for correlations.

• **Wucherer (1932),[39] [Figs. 6(e), 6(f), 7(e)]**

Tables of smoothed values based on unpublished measurements are reported by Wucherer. When comparing his original tabulated (p,T,x,y) data to other data, systematic deviations up to 0.05 in liquid mole fraction are observed, (Fig. 15).

The adjusted values, (Table 3), however, show better agreement with results of other authors. Deviations from other data sets are generally within ± 0.01 for the liquid mole fractions. At low temperatures, liquid mole fractions are about 0.02 lower than those of Postma,[22] especially at liquid mole fractions around 0.6.

Vapor mole fractions are accurate within 0.02. Due to the interpolation procedure carried out during the correction of Wucherer's data, deviations from other data are mostly systematic.

The corrected data should not be used as a basis for a correlation, but they may be useful for comparisons. Original experimental data of better quality are available overlapping Wucherer's results.

3.2.2. Saturated Liquid Densities

Deviations of saturated liquid densities from those calculated from Eq. (2) are shown for the six available sources in Fig. 9. The densities reported by Gillespie *et al.*[15] show large deviations exceeding $\pm 2\%$. Systematic deviations are also observed for the results of Jennings[17] at $x=0.8$ and those of Wachsmuth.[45] The remaining data are consistent with respect to temperature and composition within $\pm 1\%$. From the available sets of data, the measurements of Harms-Watzenberg,[29] King *et al.*,[44] and most of Jennings' results[17] for $x<0.8$ show the highest accuracy.

3.2.3. $(p,\bar{V},T,x)$ Data

$(p,\overline{V},T,x)$ data are shown separately for the liquid and vapor phases in Figs. 10 and 11. In the liquid, most data are consistent within $\pm 1\%$. The densities measured by Harms-Watzenberg[29] are probably the most reliable data, because they are internally consistent and could be represented by Eq. (2) within $\pm 0.5\%$. However, some inconsistencies are detected within this data set. Isotherms below 293 K show a systematic offset of about 0.3% in density for mole fractions $x=0.7$ and $x=0.1$. Also for $x=0.3$, systematic deviations below 293 K are observed.

The volumes of mixing determined by Staudt[47] at various temperatures and pressures have been transformed into a set of liquid densities using pure fluid densities determined from the fundamental equations of state of the pure compounds.[57,58] These densities are systematically higher than those of Harms-Watzenberg. The largest deviations occur at high ammonia mole fractions and high temperatures close to the critical locus. Here, deviations between the data of Staudt and those of Harms-Watzenberg exceed 2%.

A few densities reported by Neuhausen and Patrick[27] agree within $\pm 1\%$ with Harms-Watzenberg's data. Deviations of six densities reported by Carius[12] are also within $\pm 1\%$.

Two data sets are available for the vapor density, those measured by Ellerwald[46] and by Harms-Watzenberg.[29] Both sets were measured by the Burnett technique. Agreement is excellent, within $\pm 0.3\%$ at low pressures. Systematic deviations are observed for the highest pressures of the Burnett expansion series of Harms-Watzenberg.[29] Both sets of data are consistent with respect to composition. They are regarded as reliable and are recommended for establishing an equation of state.

3.2.4. Caloric Properties

Measurements of caloric properties are available only in the liquid phase. When including the enthalpies of the saturated liquid measured by Zinner,[48] there are four references

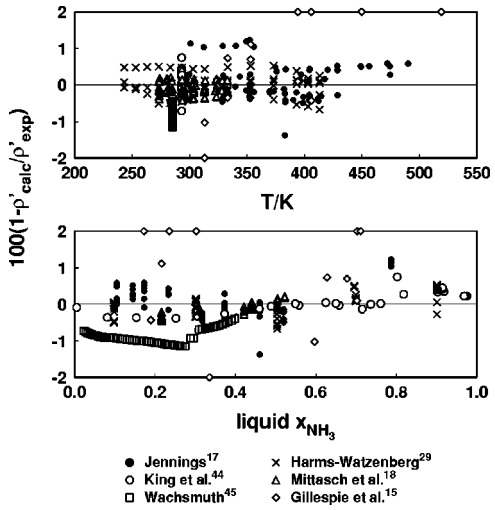

FIG. 9. Deviations between measured saturated liquid densities and values calculated from Eq. (2).

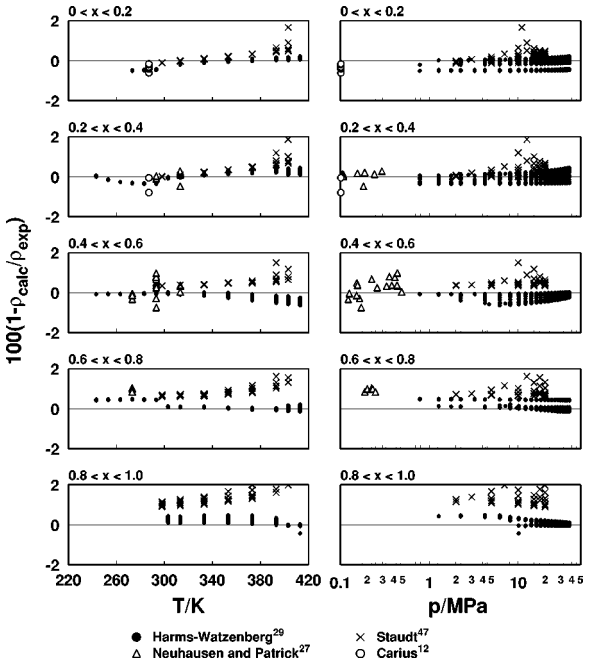

FIG. 10. Deviations between measured compressed liquid densities and values calculated from Eq. (2).

which report enthalpies and enthalpies of mixing. Isobaric heat capacities are available from three sources (see Table 1). To compare to available enthalpy measurements, enthalpies of mixing $\Delta\overline{H}$ were transformed into enthalpies according to

$$\overline{H}(T,p,x)=(1-x)\overline{H}_{01}(T,p)+x\overline{H}_{02}(T,p)+\Delta\overline{H}(T,p,x). \tag{2}$$

The pure fluid enthalpies $\overline{H}_{01}$ and $\overline{H}_{02}$ were calculated from the pure fluid equations of state. Figure 12 presents deviations of these enthalpies from Eq. (2). With the exception of the results of Macriss *et al.*,[6] all sets agree within ± 150 J/mol, which is close to the experimental uncertainty for all sets of data. The data of Macriss *et al.* show larger scatter, up to ± 300 J/mol, especially at low ammonia concentrations. Those measured at high temperatures agree better with results from other sources.

Between the measurements and values from Eq. (2), systematic deviations up to -300 J/mol are observed around $x=0.4$, while data at high ammonia mole fractions are well represented. These systematic deviations are an indicator of an inconsistency between enthalpies and other data used to establish the mixture model. Inconsistency is revealed between the enthalpies and heat capacities in the liquid in Fig. 13. Here, the heat capacity c_p is plotted versus temperature. In addition to the experimental data,[50,51] heat capacities were derived from Zinner's enthalpies. These enthalpies were fitted within ± 50 J/mol along lines of constant composition by simple temperature polynomials. Zinner's data were reported for the saturated liquid, but enthalpy is not strongly pressure-dependent in the liquid. Therefore, the values for the isobaric heat capacities obtained from the first derivative of the resulting equations should be accurate to within $\pm 1\%$.

Comparisons between experimental and derived heat capacities show a systematic offset below 290 K that increases with falling temperature. Experimental heat capacities are always lower than the derived values. At low temperatures, the derived heat capacities show an upturn for low ammonia concentrations. This behavior is also observed for pure water, especially when the equation of state of Pruss and Wagner[57] is extrapolated to lower temperatures. According to Pruss and Wagner, extrapolation gives reasonable results down to 230 K, because their equation was fitted to data in the subcooled liquid. The experimental data,[50,51] however, decrease monotonically with temperature even for low ammonia concentrations ($x \leqslant 1/3$), where an influence of the high water content and, thus, an increase of c_p with decreasing temperature might be expected.

Experience during the correlation of the mixture equation of state indicates that Zinner's results are more reliable than the heat capacities of Giauque and his co-workers. An attempt to fit these heat capacities together with $(p,\overline{V},T,x)$ data of Harms-Watzenberg[29] and (p,T,x) data of Postma[22]

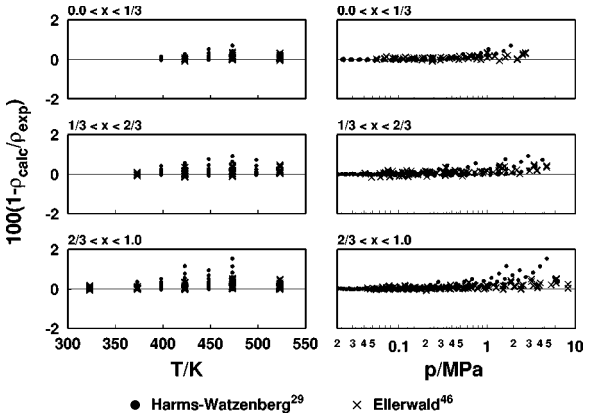

FIG. 11. Deviations between measured vapor densities and values calculated from Eq. (2).

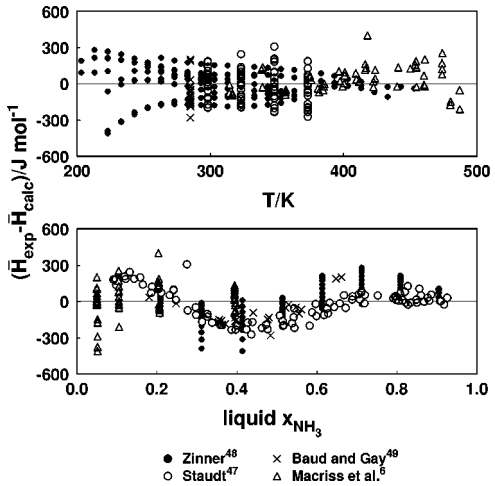

FIG. 12. Deviations between liquid enthalpies and values calculated from Eq. (2).

failed. In this case, the results of Postma showed deviations up to 0.04 of the liquid mole fraction. When the isobaric heat capacities were replaced with Zinner's enthalpies, however, a much better fit was obtained. The deviations for Postma's liquid compositions are within ± 0.02, and density deviations for Harms-Watzenberg's liquid data[29] decreased from about 1.5% to 0.3%.

Due to this experience, the enthalpy data of Zinner are recommended over the heat capacity data of Giauque and his co-workers. However, a final decision about the accuracy of either data set can be reached only when new reliable measurements of liquid heat capacities at low temperatures are available.

4. Conclusion

Comparisons of available measurements on the thermodynamic properties of {water+ammonia} have shown that the huge amount of available experimental data is far less valuable to establish an equation of state than it appears at a first glance. Most available sets of VLE data are only of limited value because they show large scatter or systematic deviations when compared to other data. Among the currently available VLE measurements, the results of Smolen *et al.*,[37] Sassen *et al.*,[25] Polak and Lu,[36] Perman,[35] and Mollier[19] are the most reliable ones in the authors' opinion. Beside these data, Postma's[22] results seem to be of reasonable quality in the low-temperature range, but they should be replaced when more accurate measurements in this range are available. To some extent, the results of Gillespie *et al.*[15] and those of Iseli[32] agree with the selected data, although their scatter is larger, especially for vapor compositions.

The largest gap in the data base is clearly found in the single-phase regions. Measurements in the vapor and, especially, in the supercritical regions are needed to establish a reliable equation of state for {water+ammonia} which is applicable beyond the critical line. Furthermore, reliable experimental data in the liquid at temperatures above 420 K and below 240 K would be highly desirable. In addition to density measurements, measurements of caloric properties are required to resolve the inconsistencies of heat capacities and enthalpies in the liquid at low temperatures.

The densities measured by Harms-Watzenberg[29] in the liquid and in the vapor and those of Ellerwald[46] seem to be the most reliable of the available single-phase data. Enthalpies of

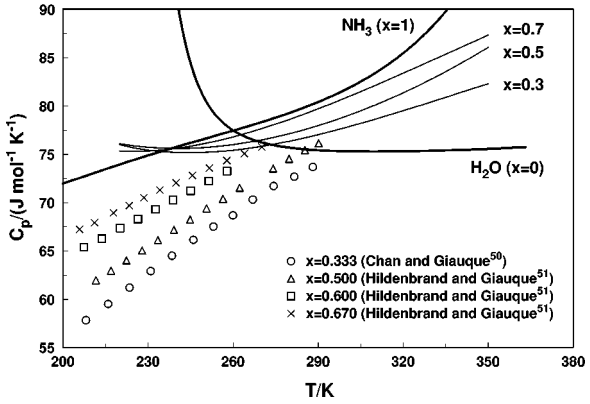

FIG. 13. Isobaric heat capacity in the liquid. $\overline{C_p}$ of NH_3 and H_2O was calculated from pure fluid equations (Refs. 57 and 58). Calculated $\overline{C_p}$ at $x=0.3$, $x=0.5$, and $x=0.7$ is derived from enthalpies of Zinner (Ref. 48).

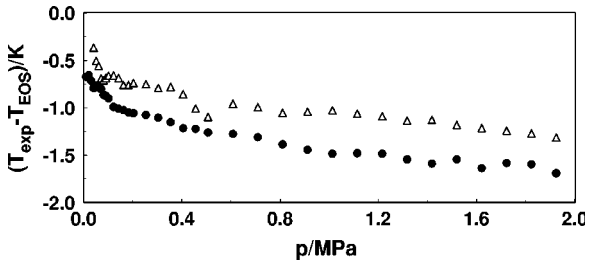

FIG. 14. Deviations of saturation temperatures for water (●) and ammonia (△) of Wucherer's (Ref. 39) original tabulation from values calculated from the pure fluid equations of state (Refs. 57 and 58).

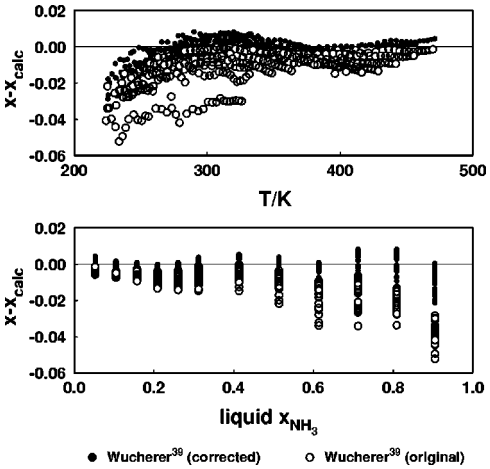

FIG. 15. Deviations of liquid mole fractions x measured by Wucherer (Ref. 39) from values calculated from Eq. (2) at tabulated values of pressure p and temperature T.

Staudt[47] and Zinner[48] are also recommended. Available heat capacities should only be considered with a very low weight for the development of an equation of state, to avoid a nonphysical behavior of the thermodynamic surface at very low temperatures.

5. Acknowledgments

The authors wish to thank A. Olson for her support during the literature survey and the update of experimental data, A. Nowarski for fruitful discussion and his help during the literature survey, and M. Kleemiβ, Institute of Thermodynamics, University Hannover, Germany for tracking down some German references from the last century. Partial support by the U.S. Department of Energy, Geothermal Division, is gratefully acknowledged.

6. Appendix: Transformations of VLE data of Wucherer[39]

Wucherer[39] reports three tables containing (p,T,x), (p,T,y), and (p,x,y) data for pressures $p<2$ MPa. In the (p,T,x) table, saturation temperatures are reported also for pure water and ammonia. These values were used to correct the given (p,T,x) values.

When Wucherer's saturation temperatures of pure water and pure ammonia are compared with results from accurate pure fluid equations of state,[57,58] temperature differences up to 1.5 K are observed (Fig. 14). These can be explained by errors occurring during temperature measurements and during the smoothing procedure leading to the tabulated data. If it is assumed that the same errors occur for the mixture measurements, Wucherer's (p,T,x) data can be corrected in the following way:

Temperature differences

$$\Delta T_{0i} = T_{0i,\mathrm{meas}} - T_{0i,\mathrm{EOS}}$$

were calculated between the pure fluid temperatures $T_{0i,\mathrm{meas}}$ and saturation temperatures $T_{0i,\mathrm{EOS}}$ obtained from the equations of state of the pure fluids. These differences were combined according to

$$\Delta T(x) = (1-x)\Delta T_{01} + x\Delta T_{02}, \qquad \text{(A1)}$$

where x is the mole fraction of ammonia and the indices 1 and 2 denote water and ammonia, respectively. The new temperature is obtained simply by subtracting the result from the reported temperature:

$$T_{\mathrm{new}}(x) = T_{\mathrm{meas}} - \Delta T(x). \qquad \text{(A2)}$$

Since the equations of state are based on ITS-90, the new temperatures also correspond to this temperature scale.

The corrected values and Wucherer's original data are compared in Fig. 15. Deviations of liquid mole fractions from those obtained from Eq. (2) are shown. The original data show deviations up to -0.06, while the corrected data are represented within ± 0.02. The corrected data agree much better with other reliable data as shown in Figs. 6(e) and 6(f).

The complete VLE information of Wucherer's data also includes the vapor composition y. A y value is obtained for each pair (p,x) from the (p,x,y) table. For (p,x) values which are not listed, y values were interpolated. Most vapor mole fractions are above 0.9, and interpolation errors should be less than the experimental uncertainty. Larger errors in y occur only for those (p,T,x,y) values with a liquid mole fraction $x<0.1$, for which y changes rapidly with pressure. The corrected (p,T,x,y) values are listed in Table 3.

7. References

[1] A. I. Kalina and M. Tribus, *Thermodynamics of the Kalina Cycle and the Need for Improved Properties Data*, Proceedings of the 12th International Conference on Properties of Water and Steam (IAPWS), edited by H. J. White *et al.* (Begell House, 1995), p. 841.
[2] F. Merkel and F. Bosnjakovic, *Diagramme und Tabellen zur Berechnung von Absorptionskältemaschinen* (Springer, Berlin, 1929).
[3] F. C. Kracek, J. Phys. Chem. **34**, 499 (1930).
[4] B. H. Jennings and F. P. Shannon, J. ASRE **35**, 333 (1938).
[5] G. Scatchard, L. F. Epstein, J. Warburton, Jr., and P. J. Cody, J. ASRE **53**, 413 (1947).
[6] R. A. Macriss, B. E. Eakin, R. T. Ellington, and J. Huebler, Physical and thermodynamic properties of ammonia-water mixtures, Res. Bull. No. **34**, Inst. of Gas Technology, Chicago (1964).
[7] B. Staples, D. Garvin, D. Smith-Magowan, J. T. L. Jobe, J. Crenka, C. R. Jackson, T. F. Wobbeking, R. Joseph, A. Brier, R. H. Schumm, and R. N. Goldberg, Bibliographies of industrial interest: Thermodynamic measurements on the systems CO_2–H_2O, $CuCl_2$–H_2O, H_2SO_4–H_2O, NH_3–H_2O, H_2S–H_2O, $ZnCl_2$–H_2O, and H_3PO_4–H_2O, No. NBS/SP-718, NBS, Gaithersburg (1986).
[8] R. A. Macriss, J. M. Gutraj, and T. S. Zawacki, Absorption fluids data survey: Final report on worldwide data, No. ONRL/Sub/84-47989/3, Institute of Gas Technology, Chicago (1988).
[9] R. A. Macriss and T. S. Zawacki, Absorption Fluids data survey: 1989 Update, No. ONRL/Sub/84-47989/4, Institute of Gas Technology, Chicago (1989).
[10] R. A. Macriss, Newsletter IEA Heat Pump Center **7**, 48 (1989).
[11] R. Tillner-Roth and D. G. Friend, J. Phys. Chem. Ref. Data **27**, 63 (1998).
[12] V. L. Carius, J. Liebigs Ann. Chem. Pharm. **99**, 129 (1856).
[13] H. W. Foote, J. Am. Chem. Soc. **43**, 1031 (1921).
[14] P. C. Gillespie, W. V. Wilding, and G. M. Wilson, Vapor liquid equilibrium measurements on the ammonia-water system from 313 K to 589 K, Res. Rep. No. 90, Gas Proc. Assoc. (1985).
[15] P. C. Gillespie, W. V. Wilding, and G. M. Wilson, AIChE Symp. Ser. **83**, 97 (1987).
[16] J.-L. Guillevic, D. Richon, and H. Renon, J. Chem. Eng. Data **30**, 332 (1985).
[17] B. H. Jennings, ASHRAE Trans. **71**, 21 (1965).
[18] A. Mittasch, E. Kuss, and H. Schlueter, Anorg. Allg. Chem. **159**, 1 (1926).
[19] H. Mollier, Z. VDI **52**, 1315 (1908).
[20] E. P. Perman, J. Chem. Soc. **79**, 718 (1901).
[21] B. Pierre, Kylt. Tidsk. Sheet **14**, 89 (1959).
[22] S. Postma, Rec. Trav. Chim. **39**, 515 (1920).
[23] S. H. Rizvi and R. A. Heidemann, J. Chem. Eng. Data **32**, 183 (1987).
[24] H. E. Roscoe and W. Dittmar, J. Liebigs Ann. Chem. Pharm. **112**, 327 (1859).
[25] C. L. Sassen, R. A. C. van Kwartel, H. J. van der Kooi, and J. de Swaan Arons, J. Chem. Eng. Data **35**, 140 (1990).

[26] T. H. Sims, J. Liebigs Ann. Chem. Pharm. **118**, 333 (1861).
[27] B. S. Neuhausen and W. A. Patrick, J. Phys. Chim. **25**, 693 (1921).
[28] I. L. Clifford and E. Hunter, J. Phys. Chem. **37**, 101 (1933).
[29] F. Harms-Watzenberg, *Messung und Korrelation der thermodynamischen Eigenschaften von Wasser-Ammoniak-Gemischen*, Fortschr.-Ber. VDI 3, No. 380 (VDI, Düsseldorf, 1995) (an additional 7 (p,T,x,y) data points were obtained from personal communication with the author).
[30] D. Hoshino, K. Nagahama, and M. Hirata, Bull. Jpn. Petrol. Inst. **17**, 9 (1975).
[31] H. Inomata, N. Ikawa, K. Arai, and S. Saito, J. Chem. Eng. Data **33**, 26 (1988).
[32] M. Iseli, Dissertation ETH Zürich, 1985.
[33] F. Kurz, Dissertation Universität Kaiserslautern, 1994.
[34] G. Müller, E. Bender, and G. Maurer, Ber. Bunsenges. Phys. Chem. **92**, 148 (1988).
[35] E. P. Perman, J. Chem. Soc. **83**, 1168 (1903).
[36] J. Polak and B. C. Y. Lu, J. Chem. Eng. Data **20**, 182 (1975).
[37] T. M. Smolen, D. B. Manley, and B. E. Poling, J. Chem. Eng. Data **36**, 202 (1991).
[38] T. A. Wilson, The total and partial vapor pressures of aqueous ammonia solutions, Bulletin No. 146, University of Illinois, Eng. Exper. Station (1925).
[39] J. Wucherer, Z. Ges. Kälteind. **39**, 97 (1932).
[40] K. Dvorak and T. Boublik, Coll. Czech. Chem. Commun. **28**, 1249 (1963).
[41] J. M. Hales and D. R. Drewes, Atmosph. Environ. **13**, 1133 (1979).
[42] M. E. Jones, J. Phys. Chem. **67**, 1113 (1963).
[43] O. A. Hougen, Chem. Mat. Eng. **32**, 704 (1925).
[44] H. H. King, J. L. Hall, and G. C. Ware, J. Am. Chem. Soc. **52**, 5128 (1930).
[45] C. Wachsmuth, Arch. Pharm. **8**, 510 (1878).
[46] M. Ellerwald, Dissertation, Universität Dortmund, 1981.
[47] H. J. Staudt, Dissertation, Universität Kaiserslautern, 1984.
[48] K. Zinner, Z. Kälteind. **41**, 21 (1934).
[49] E. Baud and L. Gay, Acad. Sci. Comptes Rend. **148**, 1327 (1909).
[50] J. P. Chan and W. F. Giauque, J. Phys. Chem. **68**, 3053 (1964).
[51] D. L. Hildenbrand and W. F. Giauque, J. Am. Chem. Soc. **75**, 2811 (1953).
[52] M. Wrewsky and A. Kaigorodoff, Z. Phys. Chem. **112**, 83 (1924).
[53] K. E. Mironov, J. Gen. Chem. USSR **25**, 1039 (1955).
[54] D. S. Tsiklis, L. R. Linshits, V. Y. Maslennikova, and N. P. Goryunova, Khim. Prom. **8**, 61 (1966).
[55] H. J. P. Bogart, *Ammonia Absorbtion Refrigeration in Industrial Processes* (Gulf, Houston, 1980).
[56] B. H. Jennings, ASHRAE Trans. **87**, 419 (1981).
[57] A. Pruβ and W. Wagner, *Eine neue Fundamentalgleichung für das fluide Zustandsgebiet von Wasser für Temperaturen von der Schmelzlinie bis zu 1273 K bei Drücken bis zu 1000 MPa*, Fortschr.-Ber. VDI 6, No. 320 (VDI, Düsseldorf, 1995).
[58] R. Tillner-Roth, F. Harms-Watzenberg, and H. D. Baehr, *Eine neue Fundamentalgleichung für Ammoniak*, Proc. 20th DKV Tagung (Heidelberg, Germany, 1993), Vol. II, p. 167.
[59] G. Baume and A. Tykociner, J. Chim. Phys. **12**, 270 (1914).
[60] L. D. Elliott, J. Phys. Chem. **28**, 887 (1924).
[61] W. Pickering, J. Chem. Soc. **63**, 181 (1891).
[62] F. F. Rupert, J. Am. Chem. Soc. **32**, 748 (1910).
[63] J. C. Rainwater and R. Tillner-Roth (unpublished).